

## Gold-carbonyl group interactions in the electrochemistry of anthraquinone thiols self-assembled on Au(111)-surfaces

Michal Wagner,\* Katrine Qvortrup, Katja E. Grier, Mikkel R. Ottosen, Jonas O. Petersen, David  
Tanner, Jens Ulstrup and Jingdong Zhang

Department of Chemistry, Technical University of Denmark, Kemitorvet, Building 207, 2800 Kgs.  
Lyngby, Denmark

E-mail: michal.wagner83@gmail.com

### Table of content

Selected STM images	Fig. S1
Plot of specific capacitance vs. applied potential	Fig. S2
Admittance-to-capacitance conversion justification	Eq. S1
Plot of Faradaic resistance vs. frequency	Fig. S3
Plots for Laviron analysis	Fig. S4-S5
Equation for calculation of apparent current density	Eq. S2
NMR spectra	Page 10-17

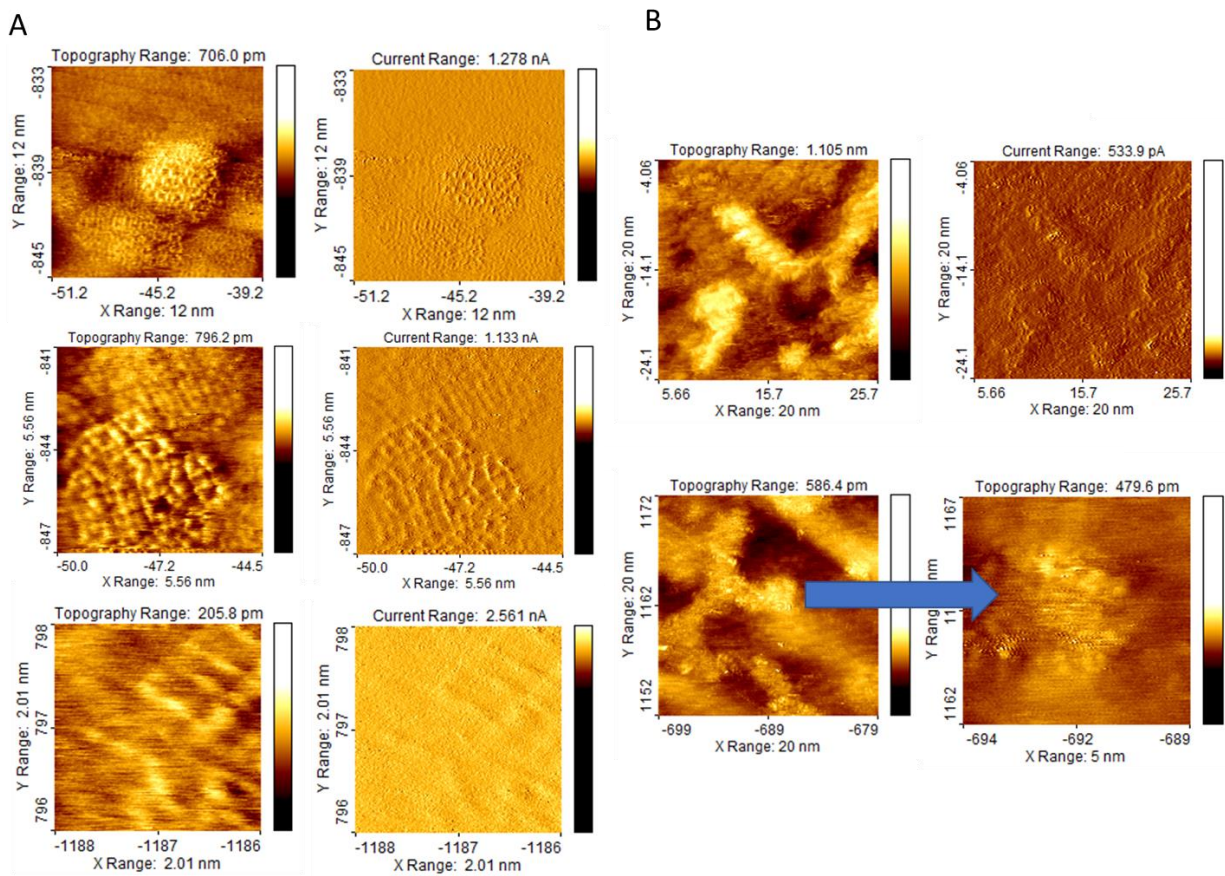


Fig. S1 An example of *ex situ* (A) and *in situ* (B) STM images of AQ2-SAMs on Au(111) electrodes. Electrolyte: 20 mM  $\text{KH}_2\text{PO}_4$  (aq) (pH = 4.75).

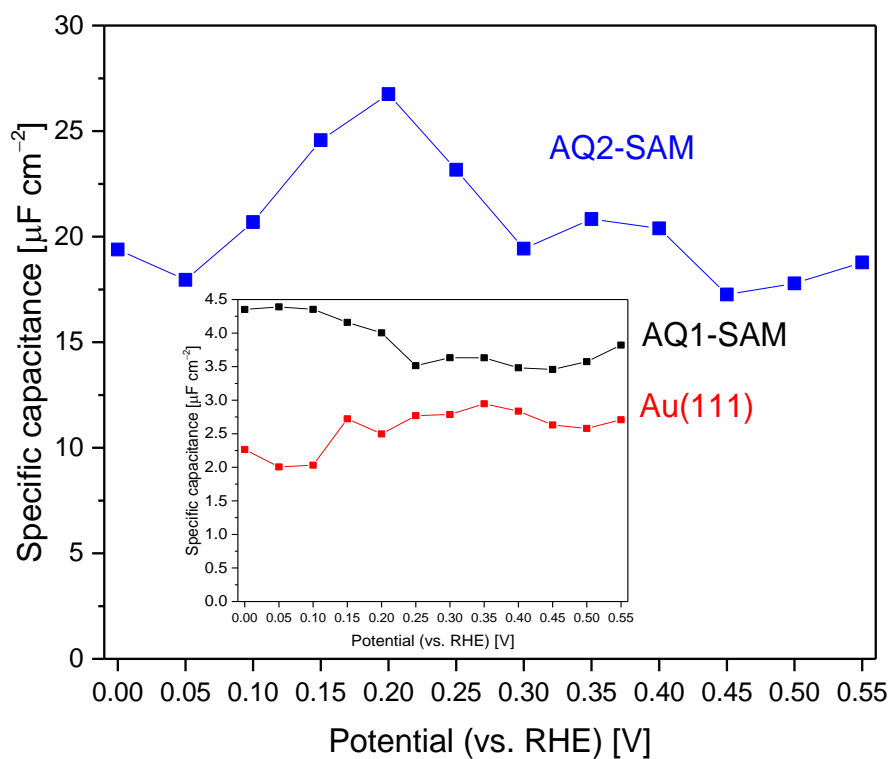


Fig. S2 Typical change in  $C_{dl}$  as a function of applied potential (pH 4.5) for bare Au(111) electrode (red), AQ1-SAM (black) and AQ2-SAM (blue).

Equation S1:

$$\text{Im}(Z_{CPE}) = \frac{1}{j\omega C} \Rightarrow C = \frac{Y_0 \omega^{n-1}}{\sin\left(\frac{n\pi}{2}\right)}$$

Since:

$$Z_{CPE} = \frac{1}{Y_0} \omega^{-n} \left[ \cos\left(-\frac{n\pi}{2}\right) + j \sin\left(-\frac{n\pi}{2}\right) \right]; j = \sqrt{-1}$$

$$\text{Im}(Z_{CPE}) = \frac{1}{Y_0} \omega^{-n} j \sin\left(-\frac{n\pi}{2}\right)$$

$$\frac{1}{Y_0} \omega^{-n} j \sin\left(-\frac{n\pi}{2}\right) = \frac{1}{j\omega C}$$

$$-\frac{1}{Y_0} \omega^{-n} \omega \sin\left(-\frac{n\pi}{2}\right) = \frac{1}{C}$$

$$\frac{1}{Y_0} \omega^{1-n} \sin\left(\frac{n\pi}{2}\right) = \frac{1}{C}$$

Thus:

$$C = \frac{Y_0 \omega^{n-1}}{\sin\left(\frac{n\pi}{2}\right)}$$

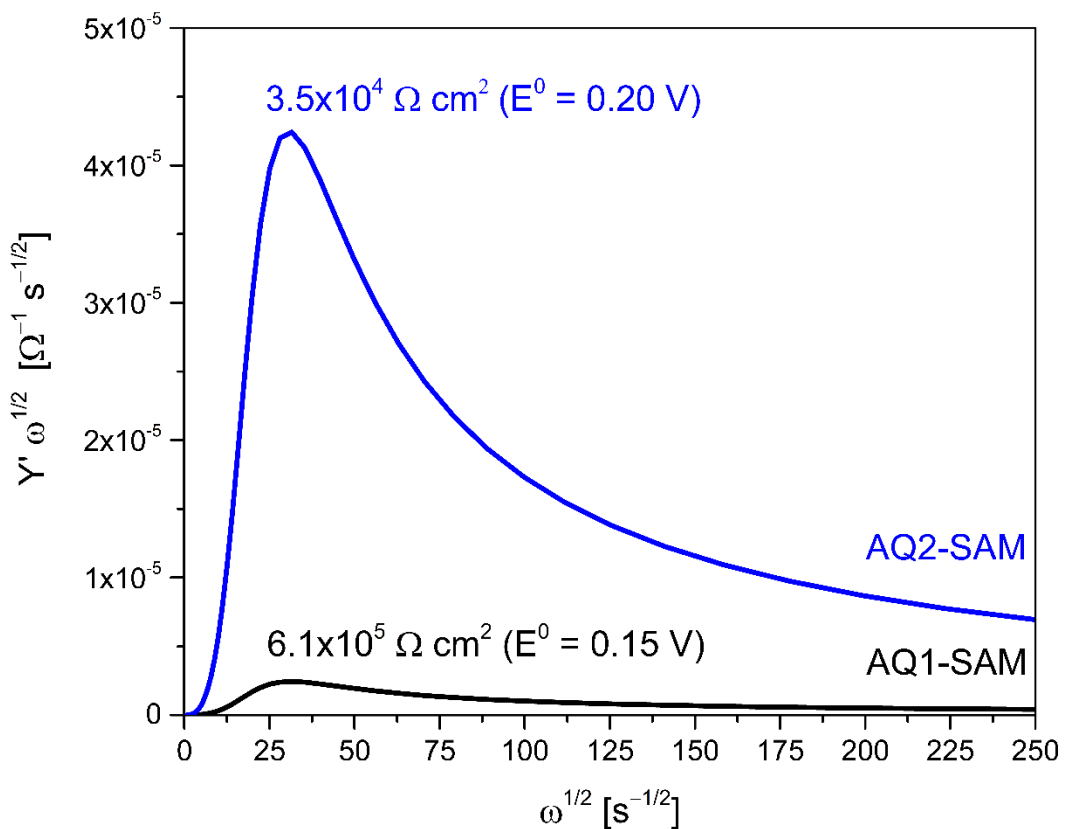


Fig. S3 Plot representing the change in real part of Faradaic admittance ( $Y'$ ) as a function of frequency for the equivalent circuit, Figure 3. The calculation was made according to the equation:  $Y' \omega^{-1/2} = \theta \sigma^{-2} \omega^{3/2} / (1 + \theta^2 \sigma^{-2} \omega^2)$ , where  $\omega$  is the angular frequency,  $1/\sigma$  is  $C_r$  and  $\theta$  is  $R_p$  [E. Laviron, *J. Electroanal. Chem.* **1979**, 105, 35-42].

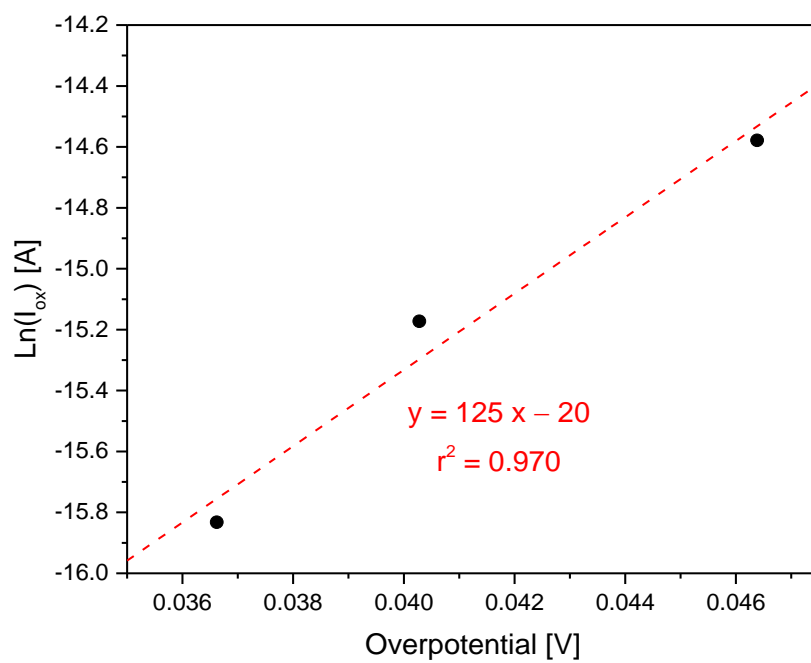


Fig. S4 Anodic current range for AQ1-SAMs at small overpotentials. The apparent  $\alpha$  value calculated from the slope of the line is *ca.* 1.6.

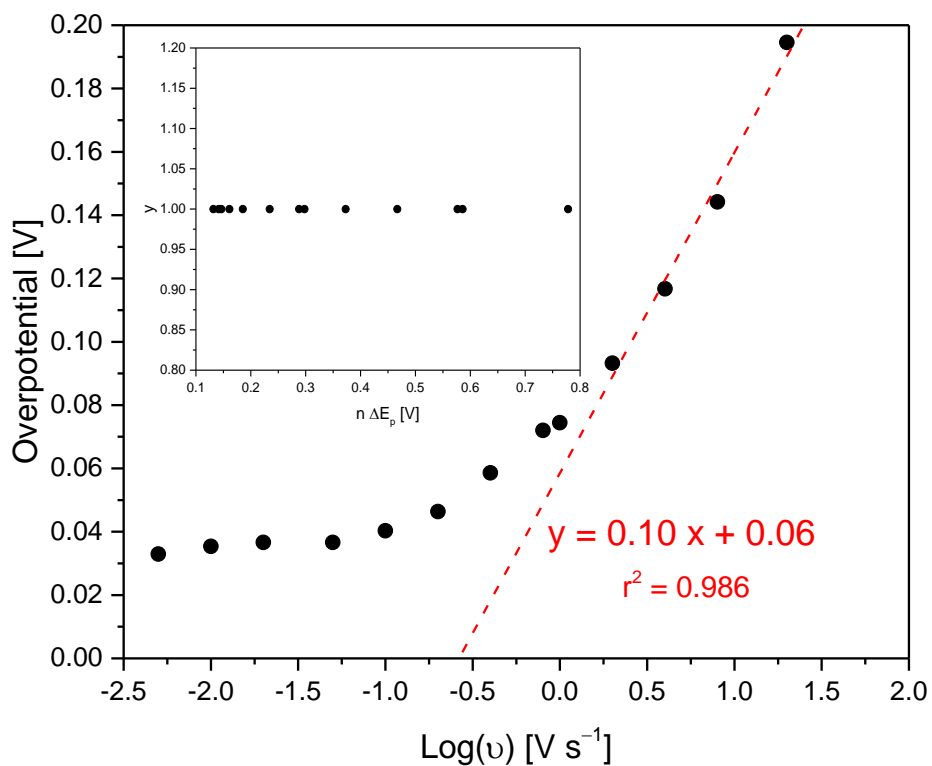


Fig. S5 Anodic range of Laviron analysis for AQ1-SAMs. Insert: variation of  $y = |\eta_{red}/\eta_{ox}|$  with peak-to-peak separation ( $\Delta E_p > 0.2/n$  V), where  $n$  is the number of electrons and  $\eta$  the overpotential. The  $\alpha$  value calculated from the slope of the line is *ca.* 0.7, which yields a  $k_s$  value of *ca.*  $6.1 \text{ s}^{-1}$ . As shown in the insert, the anodic and cathodic ranges seem very symmetric, since  $y = 1$ .

Equation S2:

$$\int_{-\infty}^{\infty} f(x)g(x)dx = \frac{1}{\sqrt{4\pi\lambda'}} \exp\left(-\frac{\lambda'}{4} - \frac{\eta'}{2}\right) \int_{-\infty}^{\infty} \exp\left(-\frac{(x-\eta')^2}{4\lambda'}\right) \frac{1}{2\cosh\left(\frac{x}{2}\right)} dx$$

where:

$$x = \frac{\varepsilon}{k_B T} \quad \lambda = \lambda' k_B T \quad e\eta = \eta' k_B T$$

The following integral:

$$\int_{-\infty}^{\infty} f(\varepsilon)g(\varepsilon) d\varepsilon = \int_{-\infty}^{\infty} H^2 \sqrt{\frac{\pi}{\lambda k_B T \hbar^2}} \exp\left(-\frac{(\lambda + e\eta - \varepsilon)^2}{4\lambda k_B T}\right) \frac{1}{1 + \exp\left(\frac{\varepsilon}{k_B T}\right)} d\varepsilon$$

Can be rearranged as:

$$Ak_B T \int_{-\infty}^{\infty} \exp\left(-\frac{(\lambda + e\eta - \varepsilon)^2}{4\lambda k_B T}\right) \frac{1}{1 + \exp\left(\frac{\varepsilon}{k_B T}\right)} d\varepsilon =$$

$$Ak_B T \int_{-\infty}^{\infty} \exp\left(-\frac{\lambda^2 + 2\lambda e\eta - 2\lambda\varepsilon + (e\eta)^2 - 2e\eta\varepsilon + \varepsilon^2}{4\lambda k_B T}\right) \frac{1}{1 + \exp\left(\frac{\varepsilon}{k_B T}\right)} d\varepsilon =$$

$$Ak_B T \int_{-\infty}^{\infty} \exp\left(-\frac{\lambda^2}{4\lambda k_B T} - \frac{2\lambda e\eta}{4\lambda k_B T} + \frac{2\lambda\varepsilon}{4\lambda k_B T} - \frac{\varepsilon^2 - 2e\eta\varepsilon + (e\eta)^2}{4\lambda k_B T}\right) \frac{1}{1 + \exp\left(\frac{\varepsilon}{k_B T}\right)} d\varepsilon =$$

$$Ak_B T \int_{-\infty}^{\infty} \exp\left(-\frac{\lambda'}{4} - \frac{\eta'}{2} + \frac{x}{2} - \frac{(x-\eta')^2}{4\lambda'}\right) \frac{1}{1 + \exp(x)} dx =$$

$$Ak_B T \int_{-\infty}^{\infty} \exp\left(-\frac{\lambda'}{4} - \frac{\eta'}{2} + \frac{x}{2}\right) \exp\left(-\frac{(x-\eta')^2}{4\lambda'}\right) \frac{1}{1 + \exp(x)} dx =$$

$$Ak_B T \int_{-\infty}^{\infty} \exp\left(-\frac{\lambda'}{4} - \frac{\eta'}{2}\right) \exp\left(\frac{x}{2}\right) \exp\left(-\frac{(x-\eta')^2}{4\lambda'}\right) \frac{1}{1 + \exp(x)} dx$$

Since, the Fermi function can be converted into:

$$\frac{1}{1 + \exp(x)} = \exp\left(-\frac{x}{2}\right) \frac{1}{2 \cosh\left(\frac{x}{2}\right)}$$

Thus:

$$A k_B T \exp\left(-\frac{\lambda'}{4} - \frac{\eta'}{2}\right) \int_{-\infty}^{\infty} \exp\left(-\frac{(x - \eta')^2}{4\lambda'}\right) \frac{1}{2 \cosh\left(\frac{x}{2}\right)} dx$$

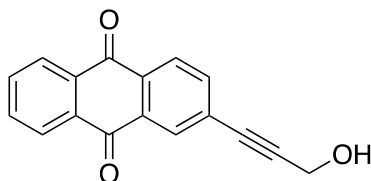
$$k_B T = k_B T \sqrt{4\pi\lambda'} \frac{1}{\sqrt{4\pi\lambda'}}$$

We therefore obtain the equation reported by S.Feldberg *Anal. Chem.* **2010**, 82, 5176–5183, and C. Chidsey *Science* **1991**, 251, 919–922:

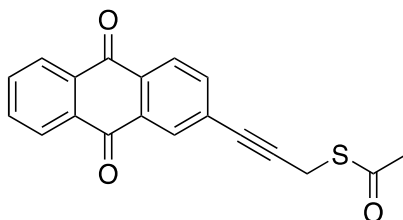
$$\frac{1}{\sqrt{4\pi\lambda'}} \exp\left(-\frac{\lambda'}{4} - \frac{\eta'}{2}\right) \int_{-\infty}^{\infty} \exp\left(-\frac{(x - \eta')^2}{4\lambda'}\right) \frac{1}{2 \cosh\left(\frac{x}{2}\right)} dx$$

Appendix with NMR spectra recorded for the following compounds:

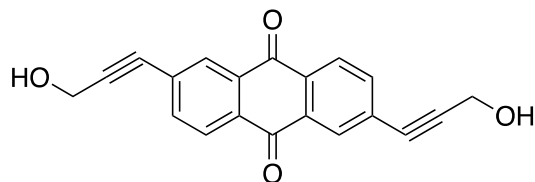
2-(3-hydroxyprop-1-yn-1-yl)anthracene-9,10-dione (**4**)



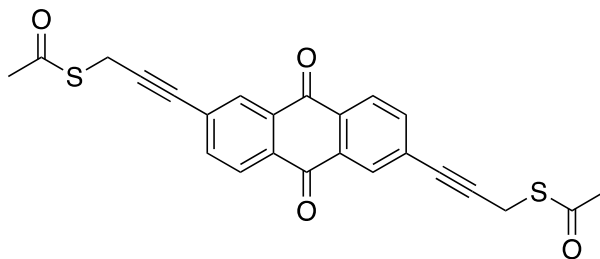
S-(3-(9,10-dioxo-9,10-dihydroanthracen-2-yl)prop-2-yn-1-yl)ethanethioate (**6**)



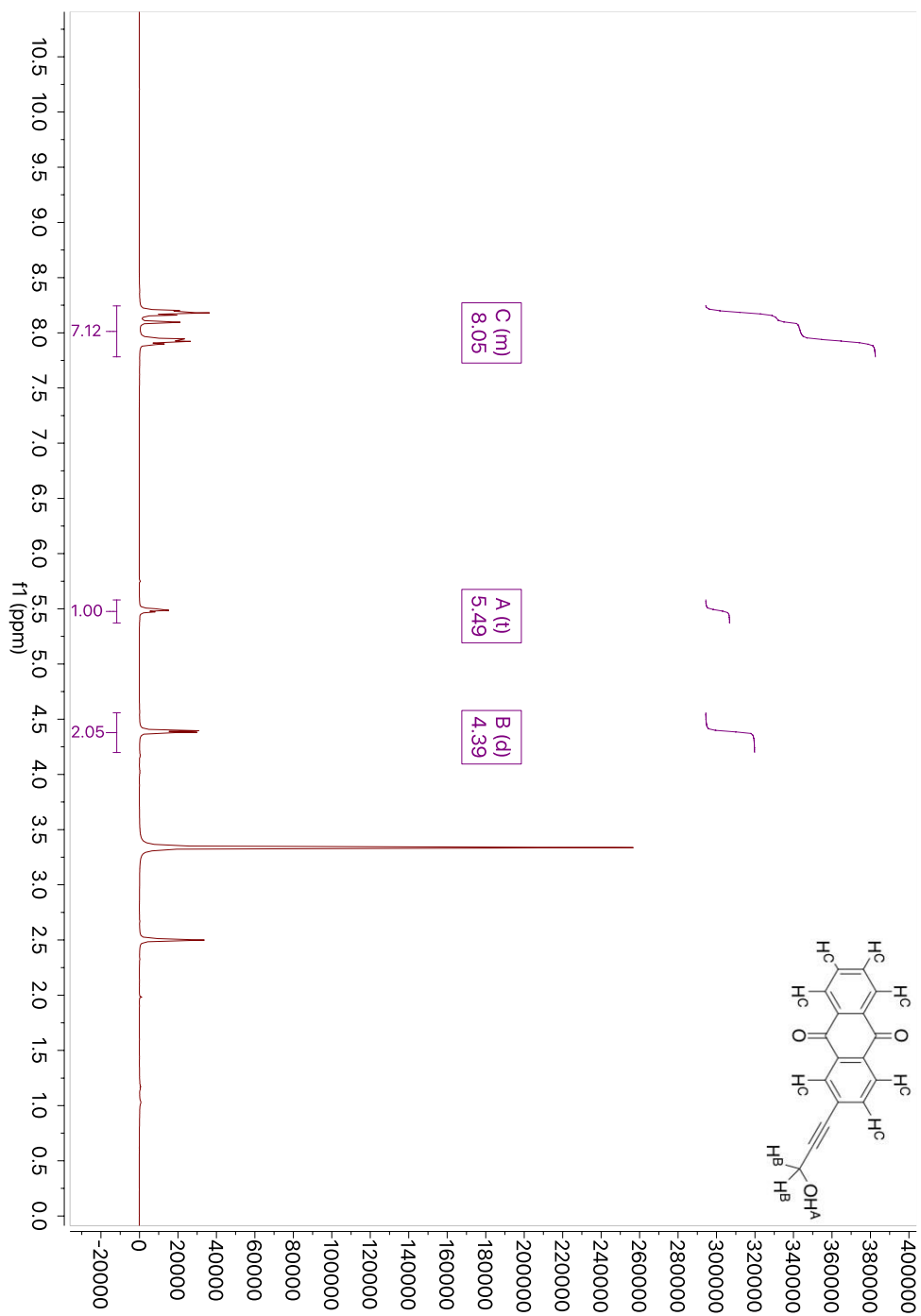
2,6-bis(3-hydroxyprop-1-yn-1-yl)anthracene-9,10-dione (**3**)



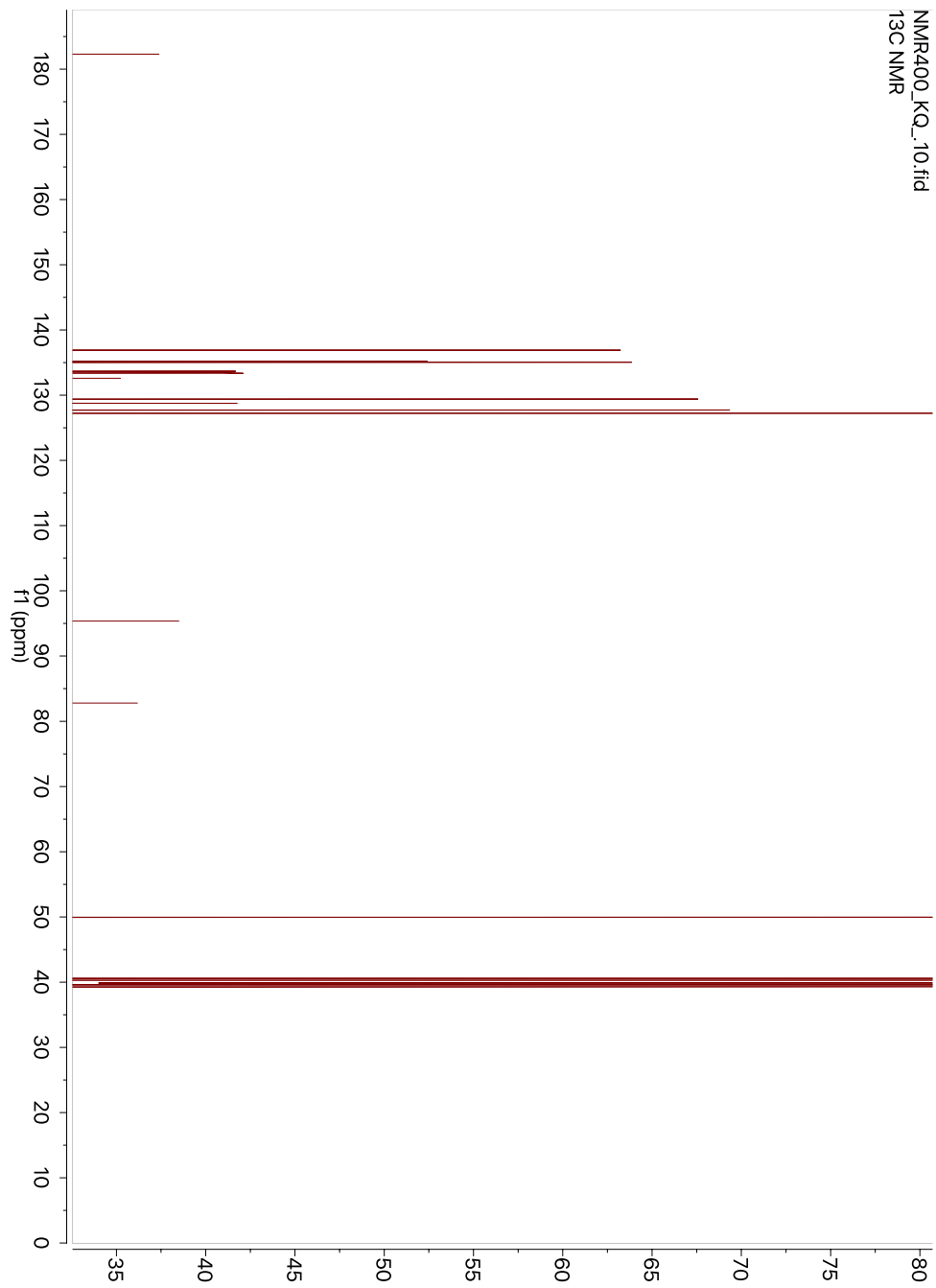
S,S'-((9,10-dioxo-9,10-dihydroanthracene-2,6-diyl)bis(prop-2-yne-3,1-diyl)) diethanethioate (**5**)



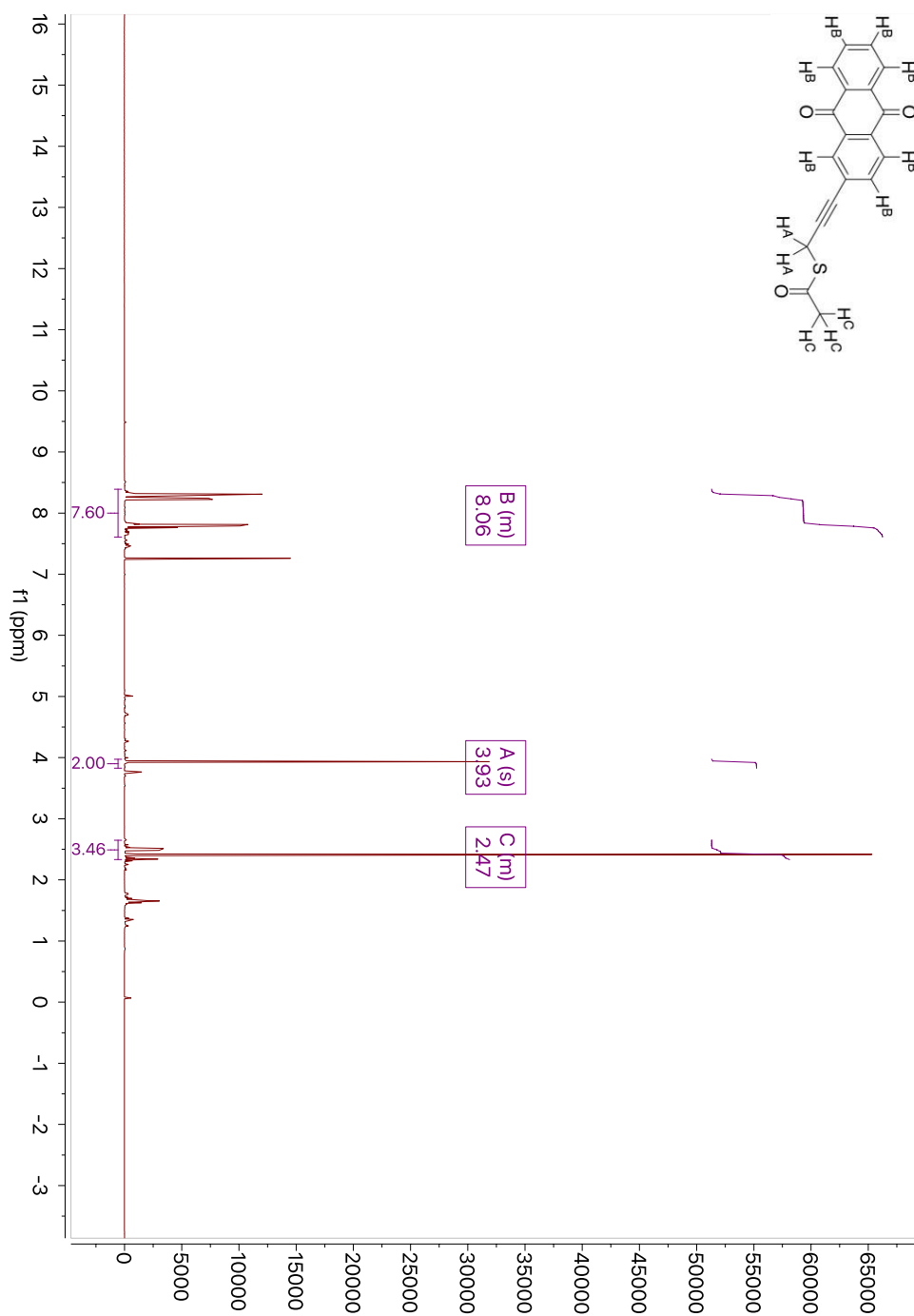
2-(3-hydroxyprop-1-yn-1-yl)anthracene-9,10-dione (**4**):  $^1\text{H-NMR}$  (400 MHz,  $\text{DMSO-}d^6$ )



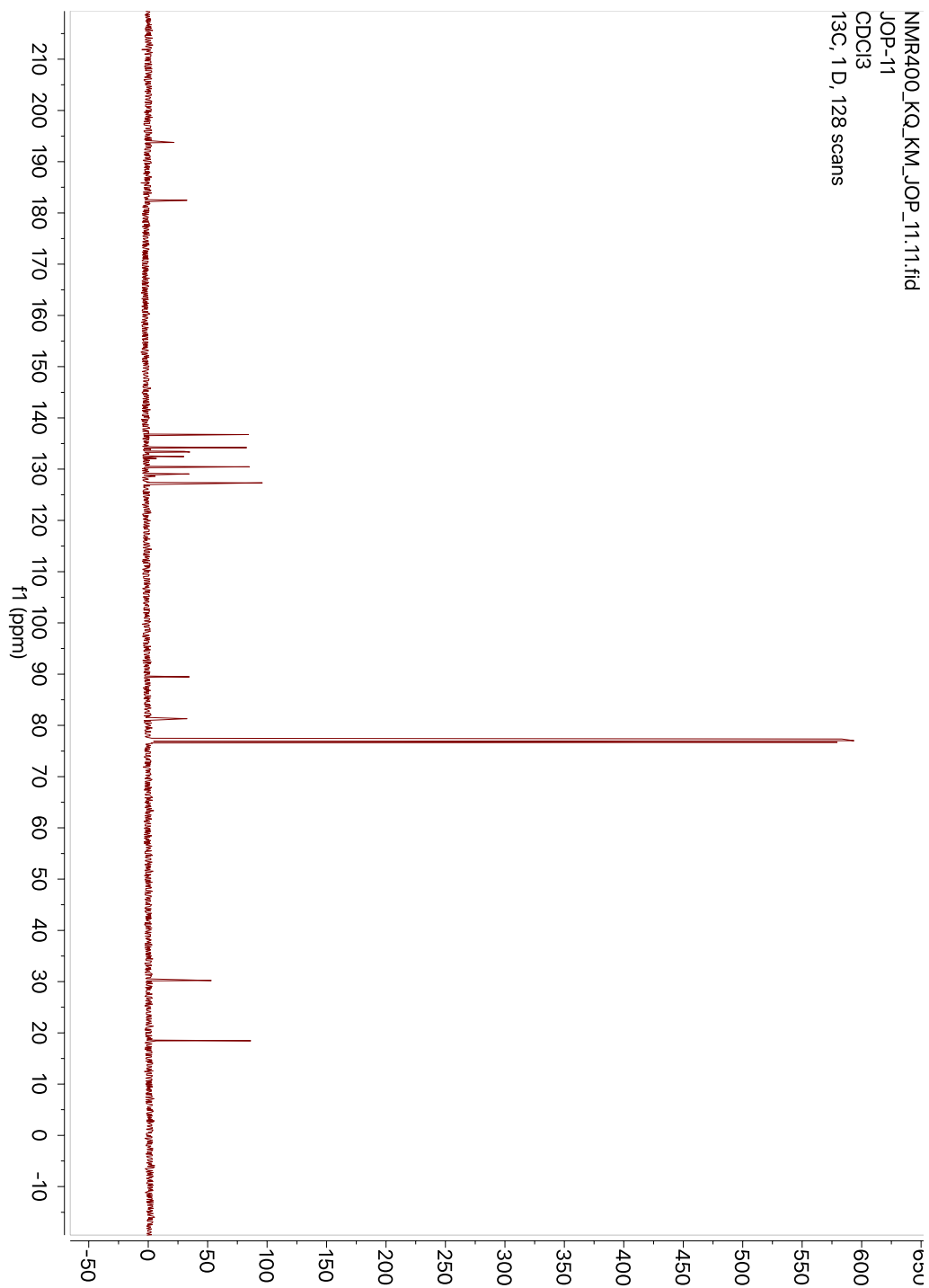
2-(3-hydroxyprop-1-yn-1-yl)anthracene-9,10-dione (**4**):  $^{13}\text{C}$ -NMR(101 MHz,  $\text{DMSO-}d_6$ )



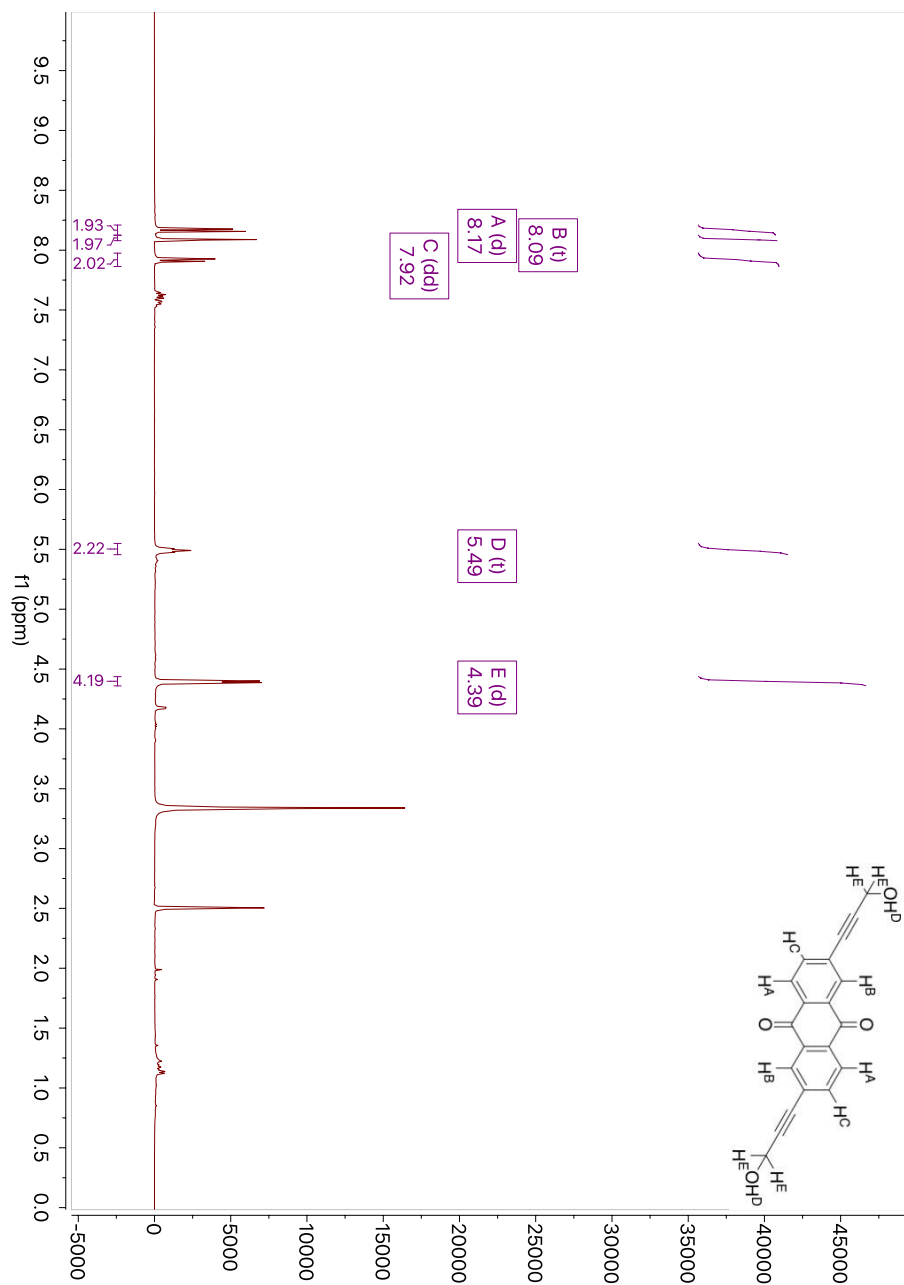
S-(3-(9,10-dioxo-9,10-dihydroanthracen-2-yl)prop-2-yn-1-yl)ethanethioate (**6**):  $^1\text{H}$  NMR (400 MHz, Chloroform-*d*)



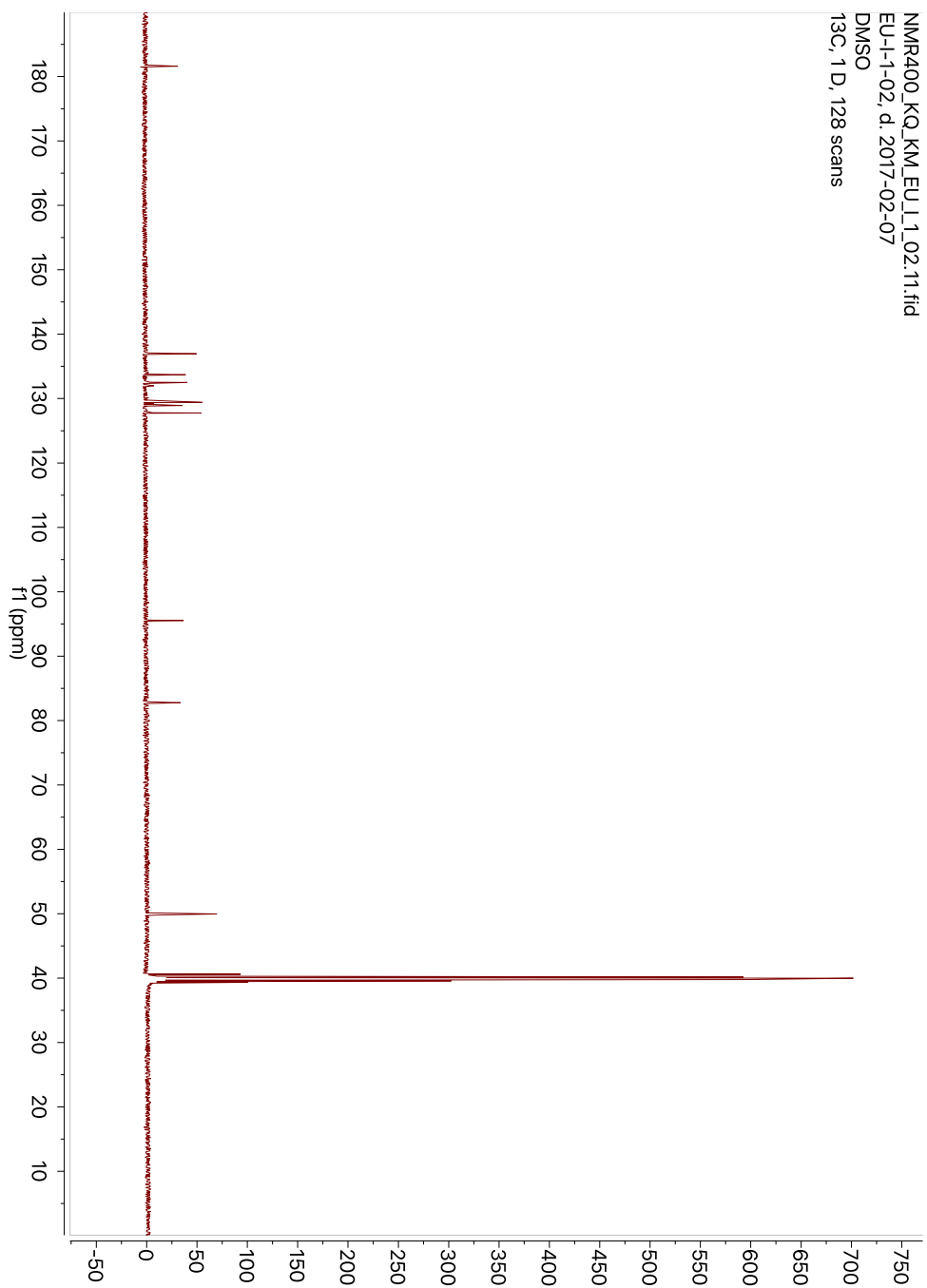
S-(3-(9,10-dioxo-9,10-dihydroanthracen-2-yl)prop-2-yn-1-yl)ethanethioate (6):  $^{13}\text{C}$  NMR (101 MHz, Chloroform-*d*)



2,6-bis(3-hydroxyprop-1-yn-1-yl)anthracene-9,10-dione (**3**):  $^1\text{H}$  NMR (400 MHz, Chloroform-*d*)



2,6-bis(3-hydroxyprop-1-yn-1-yl)anthracene-9,10-dione (**3**):  $^{13}\text{C}$  NMR (101 MHz,  $\text{DMSO-d}^6$ )



*S,S'*-((9,10-dioxo-9,10-dihydroanthracene-2,6-diyl)bis(prop-2-yne-3,1-diyl))diethanethioate  
(5):  $^1\text{H}$  NMR (400 MHz,  $\text{DMSO-}d_6$ )

